# Composites retard hydrolytic crack growth

Quan Jiao [a], Meixuanzi Shi [a,b], Tenghao Yin [a,c], Zhigang Suo [a], Joost J. Vlassak [a,*]

[a] *John A. Paulson School of Engineering and Applied Sciences, Harvard University, MA, 02138, USA*
[b] *State Key Laboratory for Strength and Vibration of Mechanical Structures, School of Aerospace Engineering, Xi'an Jiaotong University, Xi'an 710049, China*
[c] *State Key Laboratory of Fluid Power & Mechatronic System, Key Laboratory of Soft Machines and Smart Devices of Zhejiang Province, Center for X-Mechanics, and Department of Engineering Mechanics, Zhejiang University, Hangzhou 310027, China*

A R T I C L E   I N F O

A B S T R A C T

Degradable polymers are under intense development for sustainability and healthcare. Evidence has accumulated that the chemical reaction that decomposes a polymer an also grow a crack. Even under a small load, the crack speed can be orders of magnitude higher than the overall rate of degradation, leading to premature failure. Here, we demonstrate that a crack slows down markedly in a composite of two degradable materials. In a homogeneous degradable material, the stress concentrates at the crack tip, so that a relatively small applied stretch induces a high stress and a high rate of reaction. The fracture behavior of a composite that consists of two degradable materials, a stiff material for the fibers and a compliant material for the matrix, with strong adhesion between both, is different: The soft matrix blunts the crack and distributes the stresses at the crack tip over a long length of the fibers. The same rate of reaction requires a larger applied stretch. This stress de-concentration retards crack growth in the composite. We demonstrate this concept using a composite made of stiff polydimethylsiloxane (PDMS) fibers in a soft PDMS matrix. In the presence of water molecules in the environment, siloxane bonds in the PDMS hydrolyze, causing hydrolytic crack growth. We show that a hydrolytic crack grows much more slowly in a PDMS composite than in homogeneous PDMS, and may even arrest in the composite. It is hoped that this concept will contribute to the development of degradable materials that resist premature failure.

## 1. Introduction

A degradable polymer decomposes in response to a trigger, such as moisture, light, temperature, or an enzyme. Developing degradable polymers has been a fast-moving field for two principal reasons. First, the accumulation of petroleum-based plastics in the world poses an environmental challenge [1,2]. The rising concerns over plastic pollution are visibly captured by the phrase "plastic ocean" [3]. It is often said that the oceans will have more plastics than fish by 2050 [4]. Second, degradable polymers have enabled many medical applications, including drug delivery [5,6], resorbable devices [7,8], and orthopedic scaffolds [9,10].

A basic issue with degradable polymers has been identified recently. The reaction responsible for degradation of a polymer can also cause premature fracture by crack growth [11]. For example, poly(glycerol sebacate) (PGS) is a degradable polyester recently approved by the U.S. Food and Drug Administration (FDA) for biomedical applications [12,13]. Water in the environment can react with an ester bond in the PGS to form a

carboxyl group and a hydroxyl group, thus severing the chain and degrading the polymer. It was discovered recently that PGS is susceptible to hydrolytic fracture [11]. The same reaction that is responsible for degradation, hydrolysis of the ester bonds in the PGS network, can cause a crack to grow at a speed superseding the erosion rate by orders of magnitude, even when the external load is small. The crack provides a path for water molecules to reach the crack tip and the stress concentrated at the crack tip may accelerate the rate of hydrolysis. This phenomenon is believed to take place in all polymers that degrade by hydrolysis, and possibly in polymers that degrade by other chemical reactions as well. Such crack growth causes premature failure of degradable polymers. Incidentally, similar environmentally assisted crack growth has been observed in many other materials, including oxides [14–16], metals [17,18], and polymers with unsaturated carbon bonds or with siloxane bonds (e.g., natural rubber [19] and polydimethylsiloxane [20]).

Here we describe an approach to retard environmentally assisted crack growth in degradable polymers. We show that, even though a crack grows fast in a degradable polymer, a composite of two degradable polymers can retard crack growth if it consists of a stiff material for the fibers and a compliant material for

* Corresponding author.
  *E-mail address:* vlassak@seas.harvard.edu (J.J. Vlassak).

the matrix, with strong adhesion between both. For a crack in a homogeneous polymer, the stress at the crack tip concentrates to the scale of the polymer mesh size (Fig. 1a). By contrast, in the composite, the soft matrix enables the crack to blunt and distribute the stress over a long fiber segment (Fig. 1b). For the same rate of hydrolysis at the crack tip, the composite is able to sustain a larger stretch. It is this de-concentration of stress that slows down the hydrolytic crack.

We illustrate this concept using a well-known elastomer, poly-dimethylsiloxane (PDMS). PDMS is a polymer network that consists of a siloxane chains with methyl side groups (Fig. 1a), and is easier to synthesize than PGS. The methyl side groups make PDMS hydrophobic, but the siloxane bonds can react with water molecules in the environment to form silanol groups. This hydrolysis of siloxane bonds severs the polymer chains and degrades the PDMS [21]. Similar to PGS, homogeneous PDMS is susceptible to hydrolytic crack growth [20]. We demonstrate that in a composite of stiff PDMS fibers and a compliant PDMS matrix with good adhesion between both [22], cracks arrest at the matrix–fiber interface. By contrast, hydrolytic cracks grow fast in both stiff and compliant homogeneous PDMS.

## 2. Materials and methods

To test the hypothesis that a composite retards hydrolytic cracks, a commercially available PDMS precursor, Sylgard 184 (Dow Corning), is used for this study. The precursor consists of two liquids, a base and a curing agent. By changing the ratio of the two liquids, we can tune the elastic modulus of the elastomer. We use the weight ratios of 10:1 and 30:1 to prepare the "stiff" and "compliant" homogeneous PDMS, which are then used to fabricate fibers and matrix, respectively. The precursor of the stiff PDMS is mixed, degassed (Thinky ARE-250), and cast into a rectangle acrylic mold having a depth of 0.75 mm. The sample is cured in an oven (VWR Model 1410) at 65°C for 4 h. The cured film is then cut into fibers with a width of 2 mm and a length of 100 mm. The fibers are aligned in one layer in another acrylic mold with a depth of 1.5 mm. The spacing of adjacent fibers is 10 mm, and the final volume fraction of fibers in the composite is approximately 10%. The precursor of the compliant PDMS is poured into the mold and the mixture is de-gassed in a vacuum desiccator for 20 min before curing overnight at 65°C. For better visualization of the crack, both precursors are doped with less than 0.25 vol. % of a dye, yellow for the matrix and green for the fibers.

We prepare rectangular samples of the compliant, stiff, and composite PDMS. The long edges of each sample are glued to rigid clamps, so that the deforming part of the sample has a height $H = 20.0$ mm, length $L = 102.0$ mm, and thickness $B = 1.5$ mm. The two rigid clamps are pulled by a tensile tester (Instron 5966) at a constant velocity of 0.1 mm/s and the force is recorded at a frequency of 20 Hz. For the composite samples, the fibers are aligned with the direction of tension. The force divided by the cross-sectional area $LB$ in the undeformed state defines the nominal stress, $s$. The height in the deformed state divided by the original height $H$ defines the stretch, $\lambda$. Typical stress–stretch curves for the compliant, stiff, and composite PDMS obtained using this method are shown in Fig. 2a. The area under each curve yields the work per unit volume $W(\lambda)$. In this test configuration, the initial slope of each curve yields the shear modulus $\mu$, according to $s = 4\mu(\lambda - 1)$. The shear moduli of the compliant, stiff, and composite PDMS are listed in Table 1. Evidently, the ratio of the moduli of the fibers and the matrix is approximately 11.

The toughness of the compliant, stiff, and composite PDMS is measured using similar samples, except that the samples contain

**Table 1**
Mechanical properties of the compliant, stiff and composite PDMS samples.

| | Compliant PDMS | Stiff PDMS | Composite PDMS |
|---|---|---|---|
| Shear modulus (kPa) | $34 \pm 4.0$ | $377 \pm 28.0$ | $71 \pm 11.2$ |
| Toughness (J/m$^2$) | $335 \pm 39.7$ | $305 \pm 25.0$ | $993 \pm 96.2$ |

pre-cracks perpendicular to the direction of tension [23]. Pre-cracks with a length of 15 mm, are introduced in the samples using a razor blade. These samples are then tested using the same procedure as before (Fig. 2b). As the tester pulls a sample, the pre-crack blunts and then propagates across the sample at a critical stretch $\lambda_c$. The toughness is determined using $G_c = HW(\lambda_c)$, where the energy density $W(\lambda)$ is measured using a sample without pre-crack (Fig. 2c). The measured values of toughness are $335 \pm 39.7$ J/m$^2$, $305 \pm 25.0$ J/m$^2$, and $993 \pm 96.2$ J/m$^2$, for the compliant, stiff, and composite PDMS, respectively (Table 1). The composite exhibits much higher toughness than both the stiff and compliant homogeneous PDMS, as demonstrated before [22].

To study hydrolytic crack growth, a rectangular specimen with a pre-crack is held at a stretch $\lambda$ by a rigid fixture, so that the energy release rate is $G = HW(\lambda)$. The specimen is then submerged in distilled water, and the growth of the crack is recorded with a camera (Nikon D4 DSLR and Sigma 35 mm Macro lens). The resolution of the camera is better than 0.2 mm, and an image is taken every 3 to 30 min, depending on crack velocity. The velocity is calculated as crack extension divided by time interval. For cases of extremely low velocity (i.e., lower than $2 \times 10^{-8}$ m/s), the velocity is calculated using the first and the last frame only. The height of the samples of the compliant and composite PDMS is the same as before, 20.0 mm. Because stiff PDMS specimens with pre-cracks sustain less than 15% strain before fracture, we used samples with a height of 40.0 mm for this material to more easily control the stretch and to reduce experimental error. For the same reasons, we also extend the length of the pre-crack from 15 mm to 25 mm for these samples.

The analytical solution $G = HW(\lambda)$ is derived under the assumption that the length of the crack $C$ is much larger than the height $H$ of the sample. This requirement is often inconvenient in practice. We use the finite element method (ABAQUS 2016) to calculate the energy release rate when $C/H$ is small (Fig. 2d). Even for the samples with a height of 40 mm, the applied energy release rate varies only slightly over the relevant range of crack lengths. For these samples, we average the energy release rate over the center 50% of the sample resulting in a correction factor of 1.06 for the analytical energy release rate ($G = 1.06 HW(\lambda)$).

## 3. Results and discussion

We first demonstrate that homogeneous samples of both compliant and stiff PDMS are susceptible to hydrolytic cracking in an aqueous environment. The crack extension in compliant and stiff PDMS is plotted as a function of time (Fig. 3a and b). The hydrolytic crack grows continuously with time and the velocity spans approximately five orders of magnitude, depending on the applied energy release rate. The crack extension in each experiment is approximately linear with respect to time, and the average velocity of each experiment is used to construct the V–G curve (Fig. 3c). For stiff PDMS samples, at an energy release rate less than 70 J/m$^2$, no crack growth is observed after 120 h. We estimate the upper-bound velocity by dividing the measurement resolution of crack extension in our setup (i.e., 0.2 mm) by the time span of the experiment, and plot a downward arrow for each experiment in which no crack extension is observed. It is worth mentioning that the hydrolytic crack growth in PDMS has been investigated recently [20]: the crack velocity is found to be ~10
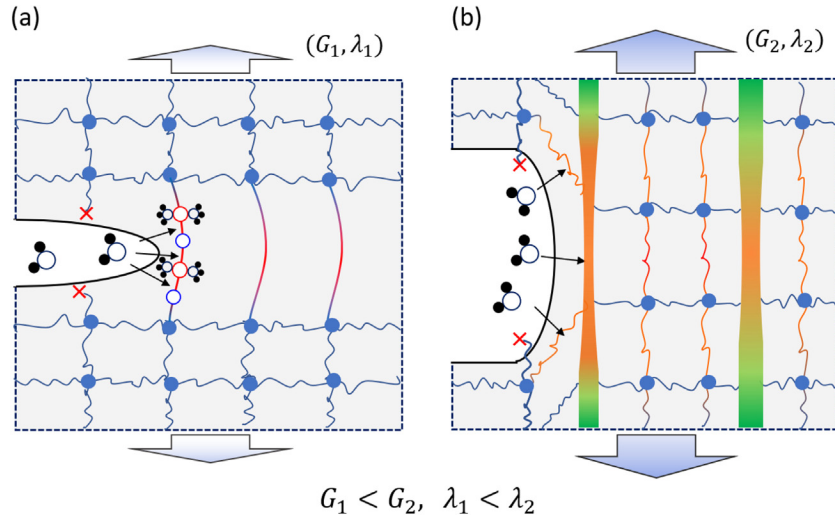
**Fig. 1.** In a moist environment, a crack in PDMS grows as the siloxane bonds in the polymer network react with water molecules to break the network. A tensile stress increases the rate of hydrolysis. (a) In homogeneous PDMS, the stress concentrates at the crack tip, so that a relatively small applied stretch induces high stress and a high rate of hydrolysis. (b) In a PDMS composite, the compliant matrix enables the crack to blunt and to de-concentrate the stress. The same rate of hydrolysis requires a larger applied stretch.
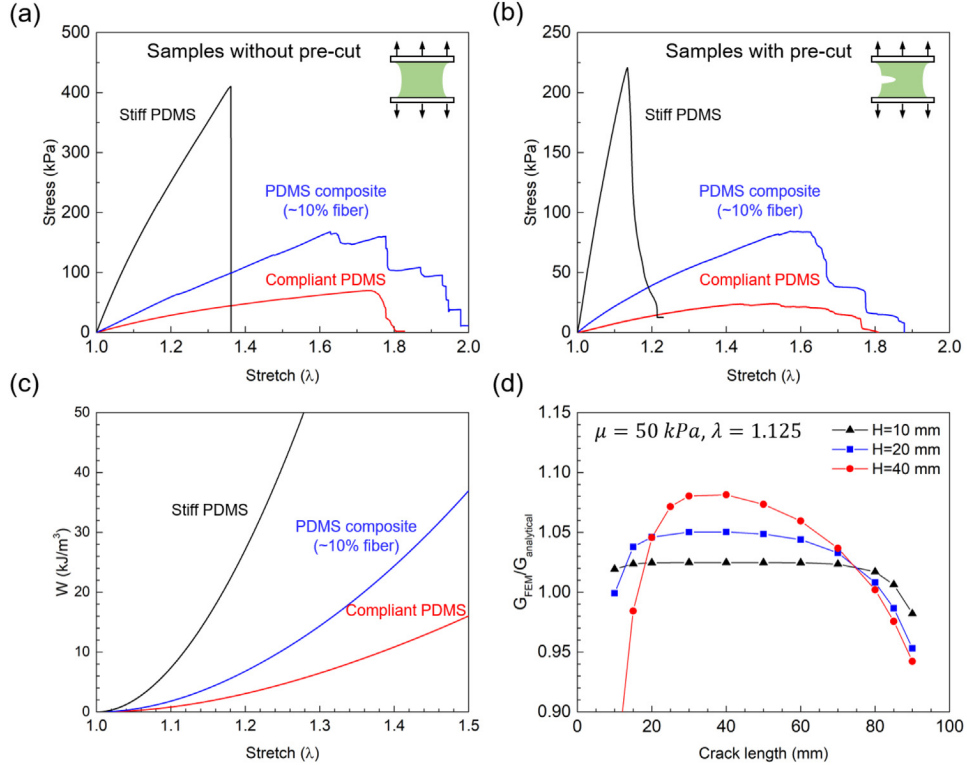


**Fig. 2.** Stress–stretch curves of PDMS samples and FEM simulations of energy release rate. (a) Stress–stretch curves of samples without pre-cut. (b) Stress–stretch curves of samples with a 15 mm pre-crack. (c) Strain energy density $W(\lambda)$ obtained by integrating the stress–strain response of PDMS samples without pre-crack.(d) Energy release rate as a function of crack length in samples with different heights calculated using FEM simulations (ABAQUS 2016). $G_{analytical}$ is calculated using $G = HW(\lambda)$, where $W(\lambda)$ is obtained by integrating the stress–strain curve of a sample with the same dimensions. $G_{FEM}$ is evaluated as a function of crack length using contour integrals.

times faster in aqueous environment than in air (RH = 11.3%) at an energy release rate of 60 J/m². We label this crack velocity ($4.5 \times 10^{-8}$ m/s) measured in low-humidity air in Fig. 3c as a reference.

Gent and co-workers showed that PDMS erodes in moist environments even under no mechanical load [21]. They measured a loss of mass of about 0.8% in humid air at 25°C after 340 h, resulting in a surface erosion rate of approximately $2.9 \times 10^{-12}$ m/s.

This value is more than two orders of magnitude lower than the lowest observed hydrolytic crack velocity (Fig. 3c). Even under a small load, a hydrolytic crack outruns surface erosion by orders of magnitude.

We proceed to examine hydrolytic crack growth in a PDMS composite. We introduce a pre-crack in the composite, with the crack tip in the matrix. We then pull the composite to a constant stretch, and record the crack extension as a function of time
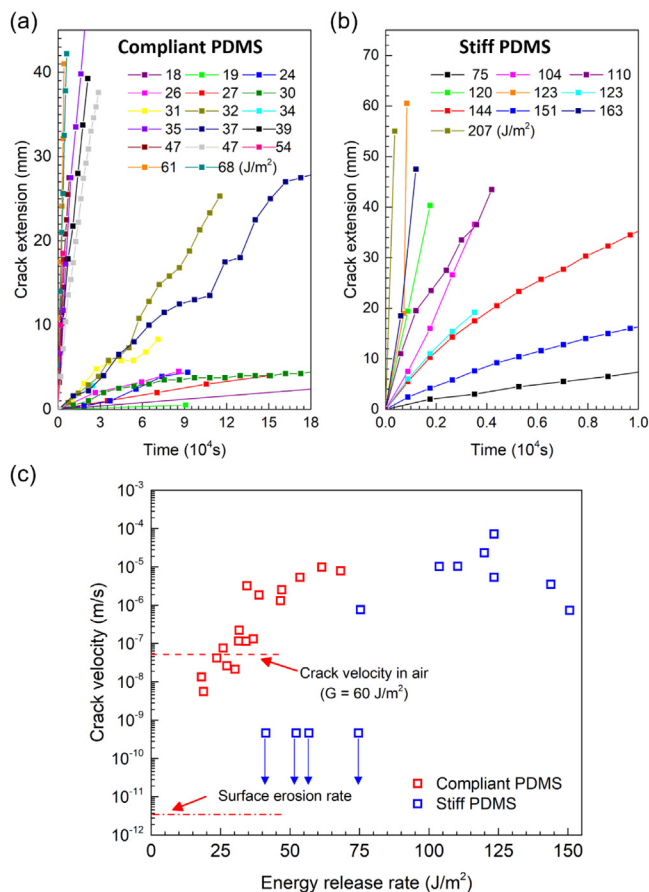
**Fig. 4.** Hydrolytic crack growth and arrest in PDMS composites. Each sample has a pre-crack with crack tip in the matrix. The sample is loaded to a value of the energy release rate and the crack extension is recorded as a function of time. For most samples tested, the crack grows and arrests at an interface between the matrix and a fiber. In each case marked by an arrow, the crack breaks a fiber, grows rapidly through the matrix, and stops at the next fiber.



**Fig. 3.** Hydrolytic crack growth in homogeneous compliant and stiff PDMS. (a) Crack growth in compliant PDMS as a function of time at various values of energy release rate. (b) Crack growth in the stiff PDMS as a function of time at various values of energy release rate. (c) Crack velocity as a function of energy release rate. The downward arrow indicates no crack growth was observed in the experiment. Also marked are the crack velocity measured in air (RH = 11.3%) at $G = 60 J/m^2$ [20] and surface erosion rate of PDMS in a moist environment [21].

(Fig. 4). The crack grows in the matrix, and arrests at the interface between the matrix and a fiber (Fig. 5a). In two experiments, however, the cracks break fibers (Fig. 5b,c). In these cases, the crack grows rapidly across the matrix, and arrests at the interface between the matrix and the next fiber. An optical micrograph of the crack tip region shows that the crack cuts the matrix around the fiber, but does not cut the fiber, and the fiber eventually stops the crack (Fig. 5b). No further breaking of fibers is observed for the entire duration of each experiment (2.5–7 days). If the applied energy release rate is sufficiently large (i.e. $\geq 242$ J/m$^2$), the large shear deformation near the crack tip develops into two short kink cracks along the matrix–fiber interface as indicated by the pair of black arrows in Fig. 5c. If the energy release rate is increased further (i.e., $\geq 447$ J/m$^2$), the kink cracks continue to grow along the fiber/matrix interface until they reach the sample grips (Fig. 5d). Thus, the composite arrests cracks at energy release rates as large as 447 J/m$^2$. This value is much higher than the threshold for the fracture of stiff PDMS ($\sim$75 J/m$^2$). Indeed, the value of 447 J/m$^2$ is even higher than the toughness of both constituent materials (Table 1).

Incidentally, at low energy release rates (e.g., 47 J/m$^2$), cracks slow down before reaching the fiber. We interpret this observation as follows. As a crack approaches a fiber, the stress concentration is progressively alleviated by the stiff fiber, which eventually arrests the crack [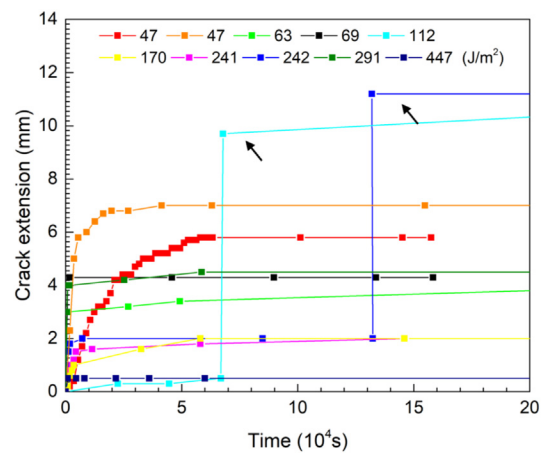24]. At more elevated energy release rates, the crack approaches the fiber quickly, but slows down as soon as it reaches the fiber and it eventually stops.

In general, under mechanical loading, a composite may fail in one of three ways: a crack may kink onto the matrix/fiber interface, break a fiber, or grow in the matrix leaving the fibers intact (Fig. 6) [25]. In our experiments, similar failure modes may be identified in a PDMS composite with a growing hydrolytic crack if the applied energy release rate is sufficiently large. The kink crack is observed only when the applied energy release rate reaches 158 J/m$^2$. The kink crack may arrest or continue to slowly propagate along the matrix/fiber interface depending on the applied energy release rate. This propagation is related to stress-assisted hydrolysis of the inter-penetrating polymer chains at the fiber/matrix interface. In the second failure mode, fiber scission may occur after the crack has arrested at the fiber for some period of time. Once the fiber breaks, the hydrolytic crack propagates rapidly through the matrix until it encounters the next fiber. The last failure mode is not observed in our experiment, probably because of good adhesion between matrix and fiber. The similarity between the failure modes observed in our experiment and in experiments carried out in a non-chemically active environments confirms the role of stress in hydrolytic crack growth.

We have shown that hydrolytic fracture slows down significantly in PDMS composites as a result of stress de-concentration at the crack tips. We suggest that this mechanics-based design to stop hydrolytic crack growth may also work for other stress-assisted chemical reactions, and thus may be of broad interest. As noted in the introduction, environmentally assisted crack growth takes place in a wide range of materials. A common strategy to retard such crack growth is to use chemical additives [26,27]. However, some of these additives have raised environmental concerns. For example, N-(1,3-dimethylbutyl)-N′-phenyl-p-phenylenediamine (6PPD) has been widely used as an antioxidant in tire rubber for decades. It was discovered only recently that 6PPD breaks down into compounds that can harm coho salmon [28]. Similar additives may raise environmental and safety concerns for degradable polymers. A mechanics-based approach to stop premature failure without the use of harmful additives may have significant benefits in this context.
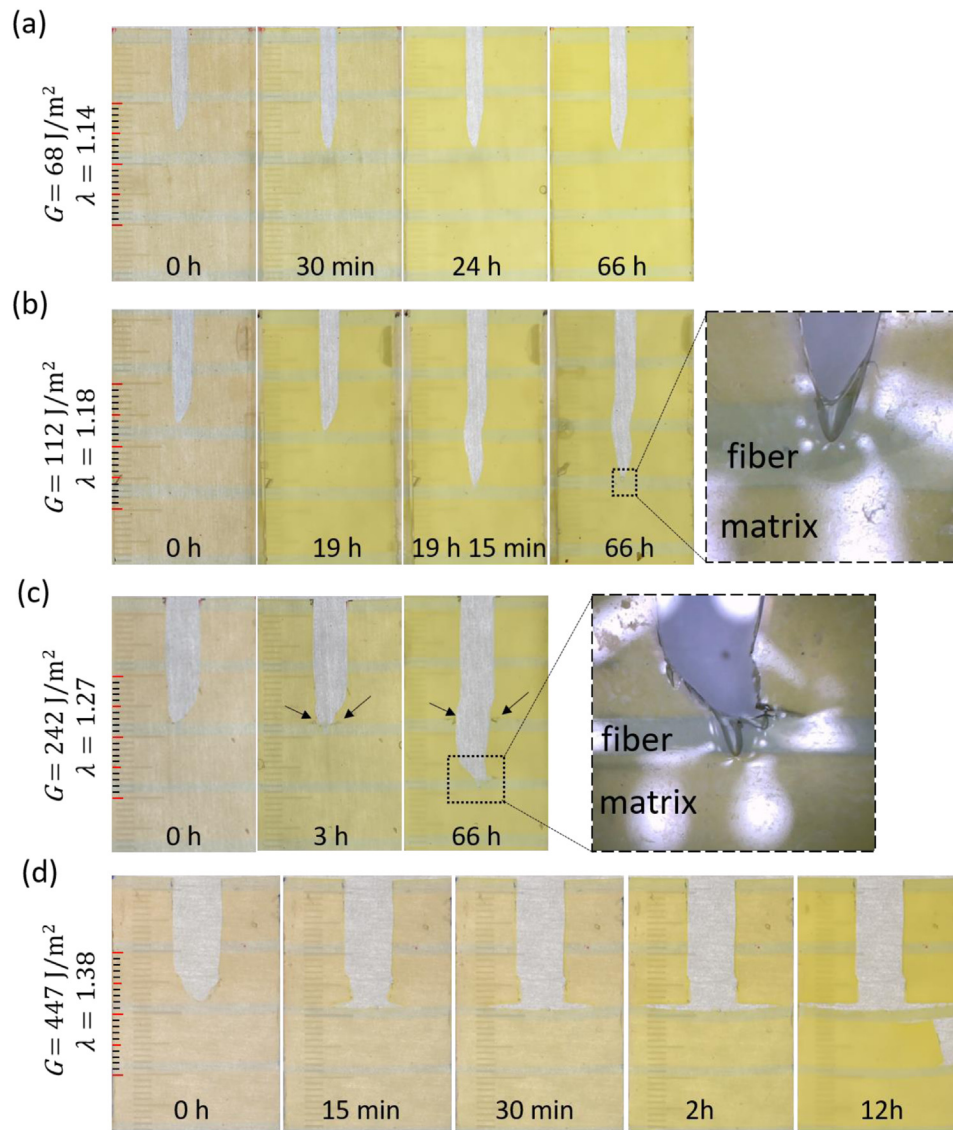
**Fig. 5.** Experimental observations of hydrolytic cracks in PDMS composites. (a) When $G = 68$ J/m$^2$, the initial crack travels 5 mm within 30 min before being arrested by the fiber. (b) When $G = 112$ J/m$^2$, the initial crack is stopped by a fiber for about 19 h before the fiber breaks. The crack rapidly grows in the matrix and is stopped by the next fiber. The micrograph shows that the crack grows in the matrix around the fiber, but the fiber remains intact and arrests the crack. (c) When $G = 242$ J/m$^2$, the initial crack reaches a fiber, kinks along the matrix/fiber interface, and arrests at the next fiber. The micrograph shows the arrested crack and kink. (d) When $G = 447$ J/m$^2$, the kinks grow along the matrix/fiber interface to the edge of the sample.
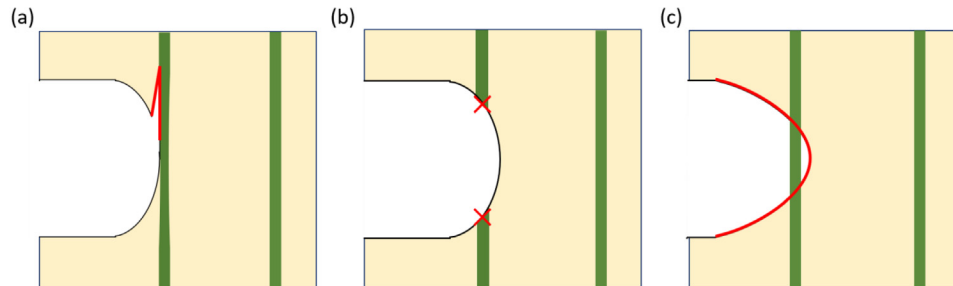


**Fig. 6.** Schematics of three failure modes of the composite. (a) A crack kinks along the matrix/fiber interface. (b) A crack breaks a fiber after being halted for a long time. (c) A crack propagates in the matrix, leaving fibers intact in its wake.

## 4. Concluding remarks

In this paper, we have explored an alternative approach to retard hydrolytic crack growth by developing composites. The composite is expected to be degradable by the same reactions as its constituents. No additives are needed. The mechanical properties (e.g., toughness, fatigue resistance) of the composite are superior to those of homogeneous materials. We have shown that the composite significantly retards hydrolytic crack growth,

even though both the matrix and fibers are susceptible to hydrolytic fracture. Under external loading, the soft matrix blunts the crack and de-concentrates stress, which slows down hydrolysis at the crack tip, and eventually arrests the hydrolytic crack. The principle is demonstrated using PDMS and implemented on a macroscopic scale. It is hoped that this approach is evaluated in various degradable polymers at different length scales.

## Declaration of competing interest

The authors declare that they have no known competing financial interests or personal relationships that could have appeared to influence the work reported in this paper.

## Acknowledgments

## References

[1] W.W.Y. Lau, Y. Shiran, R.M. Bailey, E. Cook, M.R. Stuchtey, J. Koskella, C.A. Velis, L. Godfrey, J. Boucher, M.B. Murphy, R.C. Thompson, E. Jankowska, A.C. Castillo, T.D. Pilditch, B. Dixon, L. Koerselman, E. Kosior, E. Favoino, J. Gutberlet, S. Baulch, M.E. Atreya, D. Fischer, K.K. He, M.M. Petit, U.R. Sumaila, E. Neil, M.V. Bernhofen, K. Lawrence, J.E. Palardy, Evaluating scenarios toward zero plastic pollution, Science 369 (2020) 1455–1461, http://dx.doi.org/10.1126/science.aba9475.

[2] J.R. Jambeck, R. Geyer, C. Wilcox, T.R. Siegler, M. Perryman, A. Andrady, R. Narayan, K.L. Law, Plastic waste inputs from land into the ocean, Science 347 (2015) 768–771, http://dx.doi.org/10.1126/science.1260352.

[3] F. Gallo, C. Fossi, R. Weber, D. Santillo, J. Sousa, I. Ingram, A. Nadal, D. Romano, Marine litter plastics and microplastics and their toxic chemicals components: the need for urgent preventive measures, Environ. Sci. Eur. 30 (2018) 13, http://dx.doi.org/10.1186/s12302-018-0139-z.

[4] The new plastics economy: Rethinking the future of plastics, 2021, https://www.ellenmacarthurfoundation.org/publications/the-new-plastics-economy-rethinking-the-future-of-plastics. (Accessed 27 January 2021).

[5] N. Kamaly, B. Yameen, J. Wu, O.C. Farokhzad, Degradable controlled-release polymers and polymeric nanoparticles: Mechanisms of controlling drug release, Chem. Rev. 116 (2016) 2602–2663, http://dx.doi.org/10.1021/acs.chemrev.5b00346.

[6] W.R. Gombotz, D.K. Pettit, Biodegradable polymers for protein and peptide drug delivery, Bioconjug. Chem. 6 (1995) 332–351, http://dx.doi.org/10.1021/bc00034a002.

[7] C.M. Boutry, L. Beker, Y. Kaizawa, C. Vassos, H. Tran, A.C. Hinckley, R. Pfattner, S. Niu, J. Li, J. Claverie, Z. Wang, J. Chang, P.M. Fox, Z. Bao, Biodegradable and flexible arterial-pulse sensor for the wireless monitoring of blood flow, Nat. Biomed. Eng. 3 (2019) 47–57, http://dx.doi.org/10.1038/s41551-018-0336-5.

[8] C.M. Boutry, A. Nguyen, Q.O. Lawal, A. Chortos, S. Rondeau-Gagné, Z. Bao, A sensitive and biodegradable pressure sensor array for cardiovascular monitoring, Adv. Mater. 27 (2015) 6954–6961, http://dx.doi.org/10.1002/adma.201502535.

[9] J.C. Middleton, A.J. Tipton, Synthetic biodegradable polymers as orthopedic devices, Biomaterials 21 (2000) 2335–2346, http://dx.doi.org/10.1016/S0142-9612(00)00101-0.

[10] K. Athanasiou, C. Agrawal, F. Barber, S. Burkhart, Orthopaedic applications for PLA-PGA biodegradable polymers, Arthrosc. J. Arthrosc. Relat. Surg. 14 (1998) 726–737, http://dx.doi.org/10.1016/S0749-8063(98)70099-4.

[11] M. Shi, J. Steck, X. Yang, G. Zhang, J. Yin, Z. Suo, Cracks outrun erosion in degradable polymers, Extreme Mech. Lett. 40 (2020) 100978, http://dx.doi.org/10.1016/j.eml.2020.100978.

[12] Y. Wang, G.A. Ameer, B.J. Sheppard, R. Langer, A tough biodegradable elastomer, Nat. Biotechnol. 20 (2002) 602–606, http://dx.doi.org/10.1038/nbt0602-602.

[13] R. Rai, M. Tallawi, A. Grigore, A.R. Boccaccini, Synthesis, properties and biomedical applications of poly(glycerol sebacate) (PGS): A review, Prog. Polym. Sci. 37 (2012) 1051–1078, http://dx.doi.org/10.1016/j.progpolymsci.2012.02.001.

[14] E. Orowan, The fatigue of glass under stress, Nature 154 (1944) 341–343, http://dx.doi.org/10.1038/154341a0.

[15] S.M. Wiederhorn, L.H. Bolz, Stress corrosion and static fatigue of glass, J. Am. Ceram. Soc. 53 (1970) 543–548, http://dx.doi.org/10.1111/j.1151-2916.1970.tb15962.x.

[16] E.P. Guyer, R.H. Dauskardt, Fracture of nanoporous thin-film glasses, Nature Mater. 3 (2004) 53–57, http://dx.doi.org/10.1038/nmat1037.

[17] K. Sieradzki, R.C. Newman, Brittle behavior of ductile metals during stress-corrosion cracking, Phil. Mag. A 51 (1985) 95–132, http://dx.doi.org/10.1080/01418618508245272.

[18] A. Atrens, N. Winzer, W. Dietzel, Stress corrosion cracking of magnesium alloys, Adv. Eng. Mater. 13 (2011) 11–18, http://dx.doi.org/10.1002/adem.200900287.

[19] M. Braden, A.N. Gent, The attack of ozone on stretched rubber vulcanizates. I. The rate of cut growth, J. Appl. Polym. Sci. 3 (1960) 90–99, http://dx.doi.org/10.1002/app.1960.070030713.

[20] X. Yang, J. Yang, L. Chen, Z. Suo, Hydrolytic crack in a rubbery network, Extreme Mech. Lett. 31 (2019) 100531, http://dx.doi.org/10.1016/j.eml.2019.100531.

[21] P. Vondráček, A.N. Gent, Slow decomposition of silicone rubber, J. Appl. Polym. Sci. 27 (1982) 4517–4522, http://dx.doi.org/10.1002/app.1982.070271138.

[22] Z. Wang, C. Xiang, X. Yao, P.L. Floch, J. Mendez, Z. Suo, Stretchable materials of high toughness and low hysteresis, Proc. Natl. Acad. Sci. 116 (2019) 5967–5972, http://dx.doi.org/10.1073/pnas.1821420116.

[23] R.S. Rivlin, A.G. Thomas, Rupture of rubber. I. Characteristic energy for tearing, J. Polym. Sci. 10 (1953) 291–318, http://dx.doi.org/10.1002/pol.1953.120100303.

[24] T. Ye, Z. Suo, A.G. Evans, Thin film cracking and the roles of substrate and interface, Int. J. Solids Struct. 29 (1992) 2639–2648, http://dx.doi.org/10.1016/0020-7683(92)90227-K.

[25] C. Xiang, Z. Wang, C. Yang, X. Yao, Y. Wang, Z. Suo, Stretchable and fatigue-resistant materials, Mater. Today 34 (2020) 7–16, http://dx.doi.org/10.1016/j.mattod.2019.08.009.

[26] Y. Ding, Q. Xiao, R.H. Dauskardt, Molecular design of confined organic network hybrids with controlled deformation rate sensitivity and moisture resistance, Acta Mater. 142 (2018) 162–171, http://dx.doi.org/10.1016/j.actamat.2017.09.060.

[27] J.C. Andries, D.B. Ross, H.E. Diem, Ozone attack and antiozonant protection of vulcanized natural rubber. A surface study by attenuated total reflectance spectroscopy, Rubber Chem. Technol. 48 (1975) 41–49, http://dx.doi.org/10.5254/1.3545038.

[28] Z. Tian, H. Zhao, K.T. Peter, M. Gonzalez, J. Wetzel, C. Wu, X. Hu, J. Prat, E. Mudrock, R. Hettinger, A.E. Cortina, R.G. Biswas, F.V.C. Kock, R. Soong, A. Jenne, B. Du, F. Hou, H. He, R. Lundeen, A. Gilbreath, R. Sutton, N.L. Scholz, J.W. Davis, M.C. Dodd, A. Simpson, J.K. McIntyre, E.P. Kolodziej, A ubiquitous tire rubber–derived chemical induces acute mortality in coho salmon, Science 371 (2021) 185–189, http://dx.doi.org/10.1126/science.abd6951.